Cell-Free Massive MIMO-OFDM With Low-Resolution ADCs

Özlem Tuğfe Demir*, Ahmet M. Elbir†, Emil Björnson‡
*Department of Electrical Engineering, TOBB University of Economics and Technology, Ankara, Turkiye
†Department of Electrical and Electronics Engineering, Istinye University, Istanbul, Turkiye
‡ Department of Computer Science, KTH Royal Institute of Technology, Stockholm, Sweden
E-mail: ozlemtugfedemir@etu.edu.tr, ahmetmelbir@ieee.org, emilbjo@kth.se

***Abstract*—Cell-free massive MIMO (multiple-input multiple-output) is a promising infrastructure for 6G and beyond, offering significantly higher spectral efficiency than traditional cellular systems. In cell-free massive MIMO, a large number of low-cost access points (APs) are densely deployed, making hardware impairments inevitable due to cost-effective radio hardware. While the impact of quantization and other impairments has been extensively studied for narrowband channels, their effects in wideband scenarios remain relatively unexamined. This paper presents the first analysis of how low-resolution analog-to-digital converters (ADCs) affect the uplink performance of a cell-free massive MIMO system using an orthogonal frequency division multiplexing (OFDM) waveform. Both quantization-impaired channel estimation and data detection are considered, and the quantization-unaware and quantization-aware linear receivers are developed. To further mitigate the adverse effects of quantization at the bit level, an alternating direction method of multipliers (ADMM)-based receiver is proposed. Simulation results demonstrate that the ADMM-based receiver outperforms conventional linear receivers by orders of magnitude.**

***Index Terms*—Cell-free massive MIMO, hardware impairments, low-resolution ADCs, ADMM.**

I. Introduction

Cell-free massive MIMO (multiple-input multiple-output) is a post-cellular network infrastructure in which a large number of low-cost access points (APs) are densely deployed across a network area, serving all user equipments (UEs) through coherent joint transmission and reception [1], [2]. It is considered a key enabler of ubiquitous connectivity in 6G while managing the increasing data traffic [3].

Unlike co-located massive MIMO, each AP in a cell-free system typically has relatively few antennas, as ultra-dense deployments are only viable if each AP has a minimal hardware cost. The term “massive” instead refers to the fact that the total number of AP antennas serving the UEs remains large relative to the number of UEs. Apart from having few antennas, low-cost APs suffer from hardware impairments [4]. Analyzing the impact of these impairments on communication performance is an important research direction.

The most extensively studied hardware impairment in massive MIMO systems is the use of low-resolution analog-to-digital converters (ADCs), which affect uplink performance [5]–[7]. Since the cost of ADCs increases with the number of quantization bits, understanding the adverse effects of low-resolution ADCs is crucial. While these impairments have been widely analyzed in the context of cellular massive MIMO [8], [9], studies on cell-free massive MIMO have primarily focused on narrowband channels. In practical wideband systems employing orthogonal frequency-division multiplexing (OFDM), the impact of quantization on cell-free massive MIMO performance—particularly in the presence of quantized channel estimation—remains an open question.

This paper presents a comprehensive analytical performance analysis, starting from an OFDM-based system model with quantized time-domain signals. Two channel estimation schemes are introduced: the least squares (LS) estimator, which operates without channel statistics, and the minimum mean-squared error (MMSE) estimator, which exploits statistical knowledge of the channel. For uplink data detection, two types of receive combining vectors are designed. The inner product of these vectors with the received signal vector is computed to obtain the soft estimate, which is later used for data detection. Since this preprocessing step involves linear operations, such receivers are referred to as linear receivers. To this end, both quantization-unaware and quantization-aware linear receivers are designed.

To further exploit the data structure and surpass the performance of linear receivers, an alternating direction method of multipliers (ADMM)-based receiver is proposed. Unlike linear receivers, this non-linear receiver minimizes the Euclidean distance between the quantized signal and the unknown unquantized signal at the bit level, incorporating constellation properties into the reconstruction process. By formulating the problem in a novel way, closed-form ADMM updates are derived. Simulation results demonstrate that the proposed ADMM receiver significantly enhances performance, achieving orders-of-magnitude reductions in bit error ratio (BER).

II. System Model

Consider an uplink cell-free massive MIMO with frequency-selective channels, wherein L APs and K UEs are arbitrarily distributed in the coverage area. All UEs have a single antenna, while each AP has $N \geq 1$ antennas. The complex baseband equivalent frequency-selective channel from each UE to each AP is modeled as a finite impulse response (FIR) filter with

Ö. T. Demir was supported by 2232-B International Fellowship for Early Stage Researchers Programme funded by the Scientific and Technological Research Council of Turkiye. E. Björnson was supported by the Knut and Alice Wallenberg Foundation.

ISBN 978-3-903176-73-7

R delay taps.[1] The sampling period is $T_s = 1/B$, where B is the total bandwidth of the M OFDM subcarriers with B/M subcarrier spacing.

The r-th tap of the channel from UE k to AP l is denoted by $\mathbf{h}_{kl}[r] \in \mathbb{C}^N$, for $r = 0, \ldots, R-1$. The number of subcarriers satisfies $M > R-1$, and there are $M+R-1$ samples in each OFDM symbol with a cyclic prefix (CP) length of $R-1$. The channels are assumed to be constant and take an independent realization in each coherence block consisting of n_{coh} OFDM symbols [11]. The coherence time is then $T_{\text{coh}} = n_{\text{coh}}(M+R-1)T_s$. The channels are modeled using correlated Rayleigh fading, i.e., $\mathbf{h}_{kl}[r] \sim \mathcal{N}_{\mathbb{C}}(\mathbf{0}, \mathbf{R}_{klr})$ and they are independent among different delay taps. The covariance matrix $\mathbf{R}_{klr} \in \mathbb{C}^{N \times N}$ specifies the spatial correlation of the channel $\mathbf{h}_{kl}[r]$ between the antennas of AP l and the large-scale effects such as pathloss and shadowing [8], [10], [12]. The spatial correlation matrices are fixed throughout the communication, and they are assumed known following the previous literature [2], [10], [13].

All the APs are connected to a central processing unit (CPU) via fronthaul connections. The CPU is the center point with large computational resources, and to focus on the low-resolution ADCs, we assume the fronthaul connections are error- and latency-free. In this paper, we consider centralized operation, which is the most advanced level of cell-free operation, and assume that the channel estimation and payload data detection are performed in the CPU [2, Sec. 5.1].

III. Channel Estimation

In this section, we consider the uplink channel estimation. We assume that in each coherence block, the first OFDM symbol is allocated for pilot transmission, whereas the remaining $n_{\text{coh}}-1$ OFDM symbols are used for data transmission. Now, we consider the first OFDM symbol for channel estimation. Let $\overline{\phi}_k[m]$ denote the frequency-domain pilot signal of UE k at the m-th subcarrier. The M-point inverse discrete Fourier transform (DFT) of the sequence $\overline{\phi}_k[m]$ is

$$\phi_k[q] = \frac{1}{\sqrt{M}} \sum_{m=0}^{M-1} \overline{\phi}_k[m] e^{\mathrm{j}\frac{2\pi q m}{M}}, \quad q = -(R-1), \ldots, M-1, \tag{1}$$

where we assume that a CP of length $R-1$ is appended to the time-domain samples. The baseband equivalent of the quantization-free received signal at the N antennas of AP l is

$$\breve{\mathbf{y}}_l[q] = \underbrace{\sum_{k=1}^{K}\sum_{r=0}^{R-1} \mathbf{h}_{kl}[r]\sqrt{p_k}\phi_k[q-r]}_{\triangleq \breve{\mathbf{x}}_l[q]} + \breve{\mathbf{w}}_l[q], \tag{2}$$

where $q = 0, \ldots, M-1$, p_k is the uplink transmit power of UE k, and $\breve{\mathbf{w}}_l[q] \sim \mathcal{N}_{\mathbb{C}}\left(\mathbf{0}, \sigma^2 \mathbf{I}_N\right)$ is the additive noise. The $\breve{}$ symbol is used for the pilot-related signals.

[1]Depending on the varying delay spreads between different APs and UEs, the number of taps will be different in practice. We can set the maximum number of significant delay taps as the common R without loss of generality. To simplify the analysis, a common delay tap assumption is also adopted [10].

Now, we express the quantized signal at each AP l using ADCs with arbitrary finite resolution. The real and imaginary parts of the elements of the received signal are quantized independently. Thus, it is useful to express the ADC quantization operation using real-valued variables. The $2N \times 1$ received signal at AP l before quantization can be expressed as $\breve{\mathbf{y}}_l^{\text{re}}[q] = \breve{\mathbf{x}}_l^{\text{re}}[q] + \breve{\mathbf{w}}_l^{\text{re}}[q]$ in terms of the real-valued variables

$$\breve{\mathbf{y}}_l^{\text{re}}[q] = \begin{bmatrix} \Re(\breve{\mathbf{y}}_l[q]) \\ \Im(\breve{\mathbf{y}}_l[q]) \end{bmatrix} \in \mathbb{R}^{2N}, \quad \breve{\mathbf{x}}_l^{\text{re}}[q] = \begin{bmatrix} \Re(\breve{\mathbf{x}}_l[q]) \\ \Im(\breve{\mathbf{x}}_l[q]) \end{bmatrix} \in \mathbb{R}^{2N}, \tag{3}$$

$$\breve{\mathbf{w}}_l^{\text{re}}[q] = \begin{bmatrix} \Re(\breve{\mathbf{w}}_l[q]) \\ \Im(\breve{\mathbf{w}}_l[q]) \end{bmatrix} \in \mathbb{R}^{2N}. \tag{4}$$

Let $Q(\cdot)$ denote the quantization function, which is possibly non-uniform, with b bits and $D = 2^b$ quantization levels $l_1, \ldots, l_D$. Then, the quantization function is given by

$$Q(x) = l_d \quad \text{if } x \in [\upsilon_{d-1}, \upsilon_d), \quad d = 1, \ldots, D, \tag{5}$$

where $-\infty = \upsilon_0 < \upsilon_1 < \cdots < \upsilon_{D-1} < \upsilon_D = \infty$ are the thresholds. By applying the scalar quantization function $Q(\cdot)$ to the elements of $\breve{\mathbf{y}}_l^{\text{re}}[q]$, we obtain the b-bit quantized signal as $\breve{\mathbf{d}}_l^{\text{re}}[q] = Q\left(\breve{\mathbf{y}}_l^{\text{re}}[q]\right)$, where the function acts element-wise.

For simplicity, we omit the quantization effect when implementing channel estimation. However, the quantized received signals will be utilized in the numerical results. To this end, we first collect all the unquantized time-domain signal and noise terms in vectors as

$$\breve{\mathbf{y}}_l = \begin{bmatrix} \breve{\mathbf{y}}_l[0] \\ \vdots \\ \breve{\mathbf{y}}_l[M-1] \end{bmatrix} \in \mathbb{C}^{NM}, \breve{\mathbf{w}}_l = \begin{bmatrix} \breve{\mathbf{w}}_l[0] \\ \vdots \\ \breve{\mathbf{w}}_l[M-1] \end{bmatrix} \in \mathbb{C}^{NM}. \tag{6}$$

Similarly, we collect all the time-domain channels to AP l in a single vector, i.e.,

$$\mathbf{h}_l = \left[\mathbf{h}_{1l}^{\mathrm{T}}[0] \cdots \mathbf{h}_{1l}^{\mathrm{T}}[R-1] \cdots \mathbf{h}_{Kl}^{\mathrm{T}}[0] \cdots \mathbf{h}_{Kl}^{\mathrm{T}}[R-1]\right]^{\mathrm{T}}, \tag{7}$$

which is NKR-dimensional. We also define the corresponding real-valued vectors as $\breve{\mathbf{y}}_l^{\text{re}} = [\Re(\breve{\mathbf{y}}_l)^{\mathrm{T}} \; \Im(\breve{\mathbf{y}}_l)^{\mathrm{T}}]^{\mathrm{T}}$, $\breve{\mathbf{w}}_l^{\text{re}} = [\Re(\breve{\mathbf{w}}_l)^{\mathrm{T}} \; \Im(\breve{\mathbf{w}}_l)^{\mathrm{T}}]^{\mathrm{T}}$, and $\mathbf{h}_l^{\text{re}} = [\Re(\mathbf{h}_l)^{\mathrm{T}} \; \Im(\mathbf{h}_l)^{\mathrm{T}}]^{\mathrm{T}}$. Then, the affine relationship between $\breve{\mathbf{y}}_l^{\text{re}} \in \mathbb{R}^{2NM}$ and $\mathbf{h}_l^{\text{re}} \in \mathbb{R}^{2NKR}$ becomes

$$\breve{\mathbf{y}}_l^{\text{re}} = \mathbf{M}_l \mathbf{h}_l^{\text{re}} + \breve{\mathbf{w}}_l^{\text{re}}, \tag{8}$$

where $\mathbf{M}_l \in \mathbb{R}^{2NM \times 2NKR}$ is

$$\mathbf{M}_l = \begin{bmatrix} \Re\left([\mathbf{G}_1 \cdots \mathbf{G}_K] \otimes \mathbf{I}_N\right) & -\Im\left([\mathbf{G}_1 \cdots \mathbf{G}_K] \otimes \mathbf{I}_N\right) \\ \Im\left([\mathbf{G}_1 \cdots \mathbf{G}_K] \otimes \mathbf{I}_N\right) & \Re\left([\mathbf{G}_1 \cdots \mathbf{G}_K] \otimes \mathbf{I}_N\right) \end{bmatrix}, \tag{9}$$

and

$$\mathbf{G}_k = \sqrt{p_k} \begin{bmatrix} \phi_k[0] & \phi_k[-1] & \cdots & \phi_k[-R+1] \\ \phi_k[1] & \phi_k[0] & \cdots & \phi_k[-R+2] \\ \vdots & \vdots & \vdots & \vdots \\ \phi_k[M-1] & \phi_k[M] & \cdots & \phi_k[M-R] \end{bmatrix}. \tag{10}$$

In the absence of channel statistics at APs, the simplest channel estimation scheme is the LS estimator, which is applied to the quantized signal $\breve{\mathbf{d}}_l^{\mathrm{re}}$ as

$$\widehat{\mathbf{h}}_l^{\mathrm{re}} = \mathbf{M}_l^{\dagger}\breve{\mathbf{d}}_l^{\mathrm{re}}, \tag{11}$$

where $\dagger$ denotes the pseudoinverse. The entires of $\breve{\mathbf{d}}_l^{\mathrm{re}}$ are ordered in the same way as for $\breve{\mathbf{y}}_l^{\mathrm{re}}$. If the spatial correlation matrix $\mathbf{R}_l^{\mathrm{re}} \in \mathbb{C}^{2NKR\times 2NKR}$ of $\mathbf{h}_l^{\mathrm{re}}$ is known, MMSE channel estimation can be performed to obtain

$$\widehat{\mathbf{h}}_l^{\mathrm{re}} = \mathbf{R}_l^{\mathrm{re}}\mathbf{M}_l^{\mathrm{T}}\left(\mathbf{M}_l\mathbf{R}_l^{\mathrm{re}}\mathbf{M}_l^{\mathrm{T}} + \frac{\sigma^2}{2}\mathbf{I}_{2NM}\right)^{-1}\breve{\mathbf{d}}_l^{\mathrm{re}}. \tag{12}$$

Referring to the channel vector in (7), the spatial correlation matrix $\mathbf{R}_l^{\mathrm{re}}$ can be constructed from $\mathbf{R}_{klr}$ and using the independence of the channels corresponding to different taps and UEs as

$$\mathbf{R}_l^{\mathrm{re}} = \frac{1}{2}\begin{bmatrix}\Re(\mathbf{R}_l) & -\Im(\mathbf{R}_l)\\ \Im(\mathbf{R}_l) & \Re(\mathbf{R}_l)\end{bmatrix}, \tag{13}$$

where

$$\mathbf{R}_l = \mathrm{bdiag}\left(\mathbf{R}_{1l0},\cdots,\mathbf{R}_{1l(R-1)},\cdots,\mathbf{R}_{Kl0},\cdots,\mathbf{R}_{Kl(R-1)}\right). \tag{14}$$

IV. Quantized Uplink Signal Detection

In this section, we provide the basic models for uplink signal detection. We now consider one of the OFDM symbols that are allocated for uplink data transmission. The frequency-domain uplink symbol of UE k at the m-th subcarrier is denoted by $\bar{s}_k[m]$, which has zero mean and unit power. The baseband equivalent signal transmitted from UE k at the q-th time-domain sample is given by the M-point inverse DFT of the sequence $\bar{s}_k[m]$, i.e.,

$$s_k[q] = \frac{1}{\sqrt{M}}\sum_{m=0}^{M-1}\bar{s}_k[m]e^{\mathrm{j}\frac{2\pi qm}{M}}, \quad q=-(R-1),\ldots,M-1, \tag{15}$$

where we assume that a CP of length $R-1$ is appended to the time-domain samples. The baseband equivalent of the distortion-free received signal at the N antennas of AP l is given as

$$\mathbf{y}_l[q] = \underbrace{\sum_{k=1}^{K}\sum_{r=0}^{R-1}\mathbf{h}_{kl}[r]\sqrt{p_k}s_k[q-r]}_{\triangleq\mathbf{x}_l[q]} + \mathbf{w}_l[q], \tag{16}$$

where $q=0,\ldots,M-1$, $p_k \geq 0$ is the transmission power of UE k, and $\mathbf{w}_l[q] \sim \mathcal{N}_{\mathbb{C}}\left(\mathbf{0},\sigma^2\mathbf{I}_N\right)$ is the additive noise. The received signal at AP l before quantization can be expressed as $\mathbf{y}_l^{\mathrm{re}}[q] = \mathbf{x}_l^{\mathrm{re}}[q] + \mathbf{w}_l^{\mathrm{re}}[q]$ in terms of the real-valued variables

$$\mathbf{y}_l^{\mathrm{re}}[q] = \begin{bmatrix}\Re(\mathbf{y}_l[q])\\ \Im(\mathbf{y}_l[q])\end{bmatrix} \in \mathbb{R}^{2N}, \quad \mathbf{x}_l^{\mathrm{re}}[q] = \begin{bmatrix}\Re(\mathbf{x}_l[q])\\ \Im(\mathbf{x}_l[q])\end{bmatrix} \in \mathbb{R}^{2N}, \tag{17}$$

$$\mathbf{w}_l^{\mathrm{re}}[q] = \begin{bmatrix}\Re(\mathbf{w}_l[q])\\ \Im(\mathbf{w}_l[q])\end{bmatrix} \in \mathbb{R}^{2N}. \tag{18}$$

By applying the scalar quantization function $Q(\cdot)$ to the elements of $\mathbf{y}_l^{\mathrm{re}}[q]$, we obtain the b-bit quantized signal as $\mathbf{d}_l^{\mathrm{re}}[q] = Q\left(\mathbf{y}_l^{\mathrm{re}}[q]\right)$, where the function is applied element-wise. The complex quantized signal $\dot{\mathbf{d}}_l[q] \in \mathbb{C}^N$ is given by

$$\dot{\mathbf{d}}_l[q] = \frac{1}{\sqrt{2}}Q\left(\Re(\mathbf{y}_l[q])\right) + \frac{\mathrm{j}}{\sqrt{2}}Q\left(\Im(\mathbf{y}_l[q])\right). \tag{19}$$

Taking the M-point DFT of the sequence $\dot{\mathbf{d}}_l[q] \in \mathbb{C}^N$, we obtain

$$\overline{\mathbf{d}}_l[m] = \frac{1}{\sqrt{M}}\sum_{q=0}^{M-1}\dot{\mathbf{d}}_l[q]e^{-\mathrm{j}\frac{2\pi qm}{M}}, \tag{20}$$

for $m=0,\ldots,M-1$. We can now consider data detection separately for each subcarrier. One approach to data detection is to reduce the received vector to a scalar estimate by taking its inner product with a receive combining vector. The resulting scalar is then used in a minimum-distance detector to make a decision. Since the only operation performed before detection is the inner product—a linear operation—such receivers are referred to as linear receivers. In the next section, we will explore possible linear receivers for quantized data.

V. Linear Receivers

In this section, building on [14], we develop OFDM-based extensions of the quantization-unaware and Bussgang-based quantization-aware linear receivers. Each AP l sends its distorted frequency-domain signals $\overline{\mathbf{d}}_l[m]$ to the CPU. The $LN \times 1$ overall concatenated received signal at the m-th subcarrier is

$$\overline{\mathbf{d}}[m] = \left[\overline{\mathbf{d}}_1^{\mathrm{T}}[m]\cdots\overline{\mathbf{d}}_L^{\mathrm{T}}[m]\right]^{\mathrm{T}}. \tag{21}$$

We let $\mathbf{V}[m] = [\mathbf{v}_1[m] \ \cdots \ \mathbf{v}_K[m]] \in \mathbb{C}^{LN\times K}$ denote the receive combining matrix at subcarrier m. Then, the signal for the k-th UE's data detection is given by $\mathbf{v}_k^{\mathrm{H}}[m]\overline{\mathbf{d}}[m]$, for $k=1,\ldots,K$. Next, we introduce quantization-unaware and quantization-aware linear receivers.

A. Quantization-unaware linear receivers

The quantization-unaware receivers neglect the effect of ADC quantization. Then, taking the M-point DFT of the unquantized signal $\mathbf{y}_l[q]$, we obtain

$$\begin{aligned}\overline{\mathbf{y}}_l[m] &= \frac{1}{\sqrt{M}}\sum_{q=0}^{M-1}\mathbf{y}_l[q]e^{-\mathrm{j}\frac{2\pi qm}{M}}\\ &= \sum_{k=1}^{K}\underbrace{\left(\sum_{r=0}^{R-1}\mathbf{h}_{kl}[r]e^{-\mathrm{j}\frac{2\pi rm}{M}}\right)}_{\triangleq\overline{\mathbf{h}}_{kl}[m]}\sqrt{p_k}\bar{s}_k[m]\\ &\quad + \underbrace{\frac{1}{\sqrt{M}}\sum_{q=0}^{M-1}\mathbf{w}_l[q]e^{-\mathrm{j}\frac{2\pi qm}{M}}}_{\triangleq\overline{\mathbf{w}}_l[m]}\end{aligned} \tag{22}$$

for $m=0,\ldots,M-1$. We express the concatenated unquantized signals in a compact form as

$$\underbrace{\begin{bmatrix}\overline{\mathbf{y}}_1[m]\\ \vdots\\ \overline{\mathbf{y}}_L[m]\end{bmatrix}}_{\triangleq\overline{\mathbf{y}}[m]}=\sum_{k=1}^{K}\underbrace{\begin{bmatrix}\overline{\mathbf{h}}_{k1}[m]\\ \vdots\\ \overline{\mathbf{h}}_{kL}[m]\end{bmatrix}}_{\triangleq\overline{\mathbf{h}}_k[m]}\sqrt{p_k}\overline{s}_k[m]+\underbrace{\begin{bmatrix}\overline{\mathbf{w}}_1[m]\\ \vdots\\ \overline{\mathbf{w}}_L[m]\end{bmatrix}}_{\triangleq\overline{\mathbf{w}}[m]},\quad(23)$$

where $\overline{\mathbf{w}}[m]\sim\mathcal{N}_{\mathbb{C}}(\mathbf{0},\sigma^2\mathbf{I}_{LN})$. We next make the following definitions:

$$\overline{\mathbf{H}}[m]=\left[\overline{\mathbf{h}}_1[m]\ \cdots\ \overline{\mathbf{h}}_K[m]\right]\in\mathbb{C}^{LN\times K},\quad(24)$$

$$\mathbf{P}=\mathrm{diag}(\sqrt{p_1},\ldots,\sqrt{p_K})\in\mathbb{R}^{K\times K},\quad(25)$$

$$\overline{\mathbf{s}}[m]=[\overline{s}_1[m]\ \cdots\ \overline{s}_K[m]]^{\mathrm{T}}\in\mathbb{C}^{K}.\quad(26)$$

We can then express the received signal $\overline{\mathbf{y}}[m]$ as

$$\overline{\mathbf{y}}[m]=\overline{\mathbf{H}}[m]\mathbf{P}\overline{\mathbf{s}}[m]+\overline{\mathbf{w}}[m].\quad(27)$$

We can now design the conventional receivers, which are maximum ratio combining (MRC), zero-forcing (ZF), and minimum mean-squared error (MMSE) receivers [2] as

$$\mathbf{V}_{\mathrm{MRC}}[m]=\overline{\mathbf{H}}[m]\mathbf{P},\quad(28)$$

$$\mathbf{V}_{\mathrm{ZF}}[m]=\overline{\mathbf{H}}[m]\mathbf{P}\left(\mathbf{P}\overline{\mathbf{H}}^{\mathrm{H}}[m]\overline{\mathbf{H}}[m]\mathbf{P}\right)^{-1},\quad(29)$$

$$\mathbf{V}_{\mathrm{MMSE}}[m]=\left(\overline{\mathbf{H}}[m]\mathbf{P}\mathbf{P}\overline{\mathbf{H}}^{\mathrm{H}}[m]+\sigma^2\mathbf{I}_{LN}\right)^{-1}\overline{\mathbf{H}}[m]\mathbf{P}.\quad(30)$$

B. Quantization-aware linear receivers

We consider the Bussgang decomposition [14] to express the quantized complex signal in (19) as

$$\dot{\mathbf{d}}_l[q]=\mathbf{B}_l\mathbf{y}_l[q]+\mathbf{e}_l[q],\quad(31)$$

where $\mathbf{B}_l\in\mathbb{C}^{N\times N}$ denotes the Bussgang gain matrix and $\mathbf{e}_l[q]\in\mathbb{C}^{N}$ represents the quantization distortion, which is uncorrelated with $\mathbf{y}_l[q]$ by construction. However, they are not independent. Hence, potentially better methods can be developed to exploit this dependency compared to the linear receiver, which treats the quantization distortion simply as an independent colored noise. This is the main reason which motivates us to search for alternative solutions in the next section. The Bussgang matrix $\mathbf{B}_l$ under the assumption that $\mathbf{y}_l[q]$ is Gaussian and one-bit quantization is used, i.e., $Q(x)=\mathrm{sgn}(x)$, is given by [15]

$$\mathbf{B}_l=\sqrt{\frac{2}{\pi}}\mathrm{diag}\big(\mathbf{C}_{yy,l}\big)^{-1/2},\quad(32)$$

where $\mathrm{diag}(\cdot)$ denotes the diagonal part of a matrix. The covariance matrix $\mathbf{C}_{yy,l}\in\mathbb{C}^{N\times N}$ is computed as

$$\begin{aligned}\mathbf{C}_{yy,l}&=\mathbb{E}\{\mathbf{y}_l[q]\mathbf{y}_l^{\mathrm{H}}[q]\}=\sigma^2\mathbf{I}_N\\&+\mathbb{E}\Bigg\{\sum_{k=1}^{K}\sum_{r=0}^{R-1}\mathbf{h}_{kl}[r]\sqrt{p_k}\frac{1}{\sqrt{M}}\sum_{m=0}^{M-1}\overline{s}_k[m]e^{\mathrm{j}\frac{2\pi(q-r)m}{M}}\\&\cdot\sum_{k'=1}^{K}\sum_{r'=0}^{R-1}\mathbf{h}_{k'l}^{\mathrm{H}}[r']\sqrt{p_{k'}}\frac{1}{\sqrt{M}}\sum_{m'=0}^{M-1}\overline{s}_{k'}^{*}[m']e^{-\mathrm{j}\frac{2\pi(q-r')m'}{M}}\Bigg\}\\&=\sigma^2\mathbf{I}_N+\sum_{k=1}^{K}\sum_{m=0}^{M-1}\frac{p_k}{M}\sum_{r=0}^{R-1}\sum_{r'=0}^{R-1}\mathbf{h}_{kl}[r]\mathbf{h}_{kl}^{\mathrm{H}}[r']e^{\mathrm{j}\frac{2\pi(r'-r)m}{M}}\\&=\sigma^2\mathbf{I}_N+\sum_{k=1}^{K}\frac{p_k}{M}\sum_{r=0}^{R-1}\sum_{r'=0}^{R-1}\mathbf{h}_{kl}[r]\mathbf{h}_{kl}^{\mathrm{H}}[r']\sum_{m=0}^{M-1}e^{\mathrm{j}\frac{2\pi(r'-r)m}{M}}\\&=\sum_{k=1}^{K}p_k\sum_{r=0}^{R-1}\mathbf{h}_{kl}[r]\mathbf{h}_{kl}^{\mathrm{H}}[r]+\sigma^2\mathbf{I}_N,\end{aligned}\quad(33)$$

where we have $\sum_{m=0}^{M-1}e^{\mathrm{j}\frac{2\pi(r'-r)m}{M}}=\begin{cases}M, & r=r'\\0, & r\neq r'\end{cases}$. After taking the M-point DFT and concatenating all the signals, we obtain $\overline{\mathbf{d}}[m]=\mathbf{B}\overline{\mathbf{H}}[m]\mathbf{P}\overline{\mathbf{s}}[m]+\mathbf{B}\overline{\mathbf{w}}[m]+\overline{\mathbf{e}}[m]$, where $\mathbf{B}=\mathrm{diag}(\mathbf{B}_1,\cdots,\mathbf{B}_L)\in\mathbb{C}^{LN\times LN}$, $\overline{\mathbf{e}}[m]\in\mathbb{C}^{LN}$ is the M-point DFT of $\mathbf{e}[q]=[\mathbf{e}_1^{\mathrm{T}}[q]\ \cdots\ \mathbf{e}_L^{\mathrm{T}}[q]]^{\mathrm{T}}$. Here, $\mathbf{B}\overline{\mathbf{H}}[m]\mathbf{P}\in\mathbb{C}^{LN\times K}$ is the effective channel. Such a cascade decomposition provides the best closed-form expression available. Based on this, the Bussgang-decomposition-based quantization-aware MRC (BMRC), ZF (BZF), and MMSE (BMMSE) receivers can be designed similarly to those in [14] as

$$\mathbf{V}_{\mathrm{BMRC}}[m]=\mathbf{B}\overline{\mathbf{H}}[m]\mathbf{P},\quad(34)$$

$$\mathbf{V}_{\mathrm{BZF}}[m]=\mathbf{B}\overline{\mathbf{H}}[m]\mathbf{P}\left(\mathbf{P}\overline{\mathbf{H}}^{\mathrm{H}}[m]\mathbf{B}^{\mathrm{H}}\mathbf{B}\overline{\mathbf{H}}[m]\mathbf{P}\right)^{-1},\quad(35)$$

$$\mathbf{V}_{\mathrm{BMMSE}}[m]=\left(\overline{\mathbf{C}}_{dd}[m]\right)^{-1}\mathbf{B}\overline{\mathbf{H}}[m]\mathbf{P},\quad(36)$$

where $\overline{\mathbf{C}}_{dd}[m]=\mathbb{E}\left\{\overline{\mathbf{d}}[m]\overline{\mathbf{d}}^{\mathrm{H}}[m]\right\}$ and it can be computed numerically using Monte Carlo trials. Note that $\mathbf{y}_l[q]$ is usually not Gaussian, and for an arbitrary b-bit quantization and inputs, the closed-form expressions for the matrix $\mathbf{B}$ do not exist.

VI. PROPOSED ADMM-BASED RECEIVER

We first define the following real vectors and matrix:

$$\overline{\mathbf{s}}^{\mathrm{re}}[m]=\begin{bmatrix}\Re(\overline{\mathbf{s}}[m])\\ \Im(\overline{\mathbf{s}}[m])\end{bmatrix},\quad \overline{\mathbf{y}}_l^{\mathrm{re}}[m]=\begin{bmatrix}\Re(\overline{\mathbf{y}}_l[m])\\ \Im(\overline{\mathbf{y}}_l[m])\end{bmatrix},\quad(37)$$

$$\overline{\mathbf{H}}_l^{\mathrm{re}}[m]=\begin{bmatrix}\Re(\overline{\mathbf{H}}_l[m]) & -\Im(\overline{\mathbf{H}}_l[m])\\ \Im(\overline{\mathbf{H}}_l[m]) & \Re(\overline{\mathbf{H}}_l[m])\end{bmatrix},\quad(38)$$

where $\overline{\mathbf{H}}_l[m]=\left[\overline{\mathbf{h}}_{1l}[m]\ \cdots\ \overline{\mathbf{h}}_{Kl}[m]\right]\in\mathbb{C}^{N\times K}$. Note that for the DFT of the unquantized and noise-free signal $\mathbf{x}_l^{\mathrm{re}}[q]\in\mathbb{R}^{2N}$, we can write the linear relationship

$$\overline{\mathbf{x}}_l^{\mathrm{re}}[m]=\overline{\mathbf{H}}_l^{\mathrm{re}}[m]\begin{bmatrix}\mathbf{P} & \mathbf{0}\\ \mathbf{0} & \mathbf{P}\end{bmatrix}\overline{\mathbf{s}}^{\mathrm{re}}[m].\quad(39)$$

To improve the signal detection, we will further exploit the signal structure and put a constraint on it. We then define $\mathbf{z}_{\mathrm{re}}\in\mathbb{R}^{O_{\mathrm{re}}}$ and $\mathbf{z}_{\mathrm{im}}\in\mathbb{R}^{O_{\mathrm{im}}}$ as the vectors whose entries are the possible real and imaginary parts of the considered constellation, where $O=O_{\mathrm{re}}\times O_{\mathrm{im}}$ is the constellation size. For instance, $\mathbf{z}_{\mathrm{re}}=\mathbf{z}_{\mathrm{im}}=\frac{1}{\sqrt{2}}[-1\ \ 1]^{\mathrm{T}}$ for QPSK. In this case, we can define a binary indicator vector whose entries are either zero or one, but only one entry is one, which corresponds to the real or imaginary part of symbol entry in $\mathbf{z}_{\mathrm{re}}$ and $\mathbf{z}_{\mathrm{im}}$. We let $\mathbf{b}[m]\in\mathbb{R}^{K(O_{\mathrm{re}}+O_{\mathrm{im}})}$ denote this binary vector for the mth subcarrier symbols. We can then express the relation between $\overline{\mathbf{s}}^{\mathrm{re}}[m]$ and $\mathbf{b}[m]$ as $\overline{\mathbf{s}}^{\mathrm{re}}[m] = \begin{bmatrix} \mathbf{I}_K \otimes \mathbf{z}_{\mathrm{re}}^{\mathrm{T}} & \mathbf{0} \\ \mathbf{0} & \mathbf{I}_K \otimes \mathbf{z}_{\mathrm{im}}^{\mathrm{T}} \end{bmatrix} \mathbf{b}[m]$, with the additional constraints

$$[\mathbf{b}[m]]_j \in \{0,1\}, \quad j = 1, \ldots, K(O_{\mathrm{re}} + O_{\mathrm{im}}), \tag{40}$$

$$\sum_{j=O_{\mathrm{re}}(k-1)+1}^{O_{\mathrm{re}}k} [\mathbf{b}[m]]_j = 1, \quad k = 1, \ldots, K, \tag{41}$$

$$\sum_{j=KO_{\mathrm{re}}+O_{\mathrm{im}}(k-1)+1}^{KO_{\mathrm{re}}+O_{\mathrm{im}}k} [\mathbf{b}[m]]_j = 1, \quad k = 1, \ldots, K. \tag{42}$$

Then, the linear relation in (39) can be expressed as

$$\overline{\mathbf{x}}_l^{\mathrm{re}}[m] = \underbrace{\overline{\mathbf{H}}_l^{\mathrm{re}}[m] \begin{bmatrix} \mathbf{P} & \mathbf{0} \\ \mathbf{0} & \mathbf{P} \end{bmatrix} \begin{bmatrix} \mathbf{I}_K \otimes \mathbf{z}_{\mathrm{re}}^{\mathrm{T}} & \mathbf{0} \\ \mathbf{0} & \mathbf{I}_K \otimes \mathbf{z}_{\mathrm{im}}^{\mathrm{T}} \end{bmatrix}}_{\triangleq \mathbf{A}_{l,m} \in \mathbb{R}^{2N \times K(O_{\mathrm{re}}+O_{\mathrm{im}})}} \mathbf{b}[m]. \tag{43}$$

Now, using these constraints, we cast an optimization problem with the objective of minimizing the Euclidean distance between the DFT of the quantized noisy signal, $\overline{\mathbf{d}}_l^{\mathrm{re}}[m] = \left[\Re\left(\overline{\mathbf{d}}_l^{\mathrm{T}}[m]\right), \Im\left(\overline{\mathbf{d}}_l^{\mathrm{T}}[m]\right)\right]^{\mathrm{T}}$ and unknown unquantized noise-free signal $\overline{\mathbf{x}}_l^{\mathrm{re}}[m]$. The optimization problem is written as

$$\underset{\overline{\mathbf{x}}_l^{\mathrm{re}}[m], \mathbf{b}[m] \forall l,m}{\text{minimize}} \quad \sum_{l=1}^{L} \sum_{m=0}^{M-1} \left\| \overline{\mathbf{x}}_l^{\mathrm{re}}[m] - \overline{\mathbf{d}}_l^{\mathrm{re}}[m] \right\|^2 \tag{44a}$$

$$\text{subject to} \quad \overline{\mathbf{x}}_l^{\mathrm{re}}[m] = \mathbf{A}_{l,m} \mathbf{b}[m], \quad \forall l, m \tag{44b}$$

$$\mathbf{b}_1[m] = \mathbf{b}[m], \quad [\mathbf{b}_1[m]]_j \in \{0,1\}, \quad \forall j, m \tag{44c}$$

$$\mathbf{b}_2[m] = \mathbf{b}[m], \quad \sum_{j=O_{\mathrm{re}}(k-1)+1}^{O_{\mathrm{re}}k} [\mathbf{b}_2[m]]_j = 1, \quad \forall k, m \tag{44d}$$

$$\sum_{j=KO_{\mathrm{re}}+O_{\mathrm{im}}(k-1)+1}^{KO_{\mathrm{re}}+O_{\mathrm{im}}k} [\mathbf{b}_2[m]]_j = 1, \quad \forall k, m, \tag{44e}$$

where we have created two copies of $\mathbf{b}[m]$ to prepare for an ADMM solution with closed-form updates. In this paper, we use the ADMM as a heuristic since the above problem is non-convex. The proposed ADMM-based receiver operates at the bit level, whereas previous linear receivers function at the block level, applying the same combining vectors to all symbols within a coherence block.

A. Closed-Form ADMM Updates

The steps of the ADMM algorithm in scaled form [16] at the ith iteration are given as follows:

$$\begin{aligned} \overline{\mathbf{x}}_l^{\mathrm{re}(i+1)}[m] \leftarrow \underset{\overline{\mathbf{x}}_l^{\mathrm{re}}[m]}{\arg\min} \quad & \left\| \overline{\mathbf{x}}_l^{\mathrm{re}}[m] - \overline{\mathbf{d}}_l^{\mathrm{re}}[m] \right\|^2, \\ & + \rho \left\| \overline{\mathbf{x}}_l^{\mathrm{re}}[m] - \mathbf{A}_{l,m} \mathbf{b}^{(i)}[m] + \mathbf{u}_l^{(i)}[m] \right\|^2, \quad \forall l, \end{aligned} \tag{45}$$

$$\begin{aligned} \mathbf{b}_1^{(i+1)}[m] \leftarrow \underset{\mathbf{b}_1[m]}{\arg\min} \quad & \rho \left\| \mathbf{b}_1[m] - \mathbf{b}^{(i)}[m] + \tilde{\mathbf{u}}_1^{(i)}[m] \right\|^2 \\ \text{subject to} \quad & [\mathbf{b}_1[m]]_j \in \{0,1\}, \quad \forall j, \end{aligned} \tag{46}$$

$$\begin{aligned} \mathbf{b}_2^{(i+1)}[m] \leftarrow \underset{\mathbf{b}_2[m]}{\arg\min} \quad & \rho \left\| \mathbf{b}_2[m] - \mathbf{b}^{(i)}[m] + \tilde{\mathbf{u}}_2^{(i)}[m] \right\|^2 \\ \text{subject to} \quad & \sum_{j=O_{\mathrm{re}}(k-1)+1}^{O_{\mathrm{re}}k} [\mathbf{b}_2[m]]_j = 1, \quad \forall k \\ & \sum_{j=KO_{\mathrm{re}}+O_{\mathrm{im}}(k-1)+1}^{KO_{\mathrm{re}}+O_{\mathrm{im}}k} [\mathbf{b}_2[m]]_j = 1, \quad \forall k, \end{aligned} \tag{47}$$

$$\begin{aligned} & \mathbf{b}^{(i+1)}[m] \leftarrow \\ & \underset{\mathbf{b}[m]}{\arg\min} \quad \rho \sum_{l=1}^{L} \left\| \overline{\mathbf{x}}_l^{\mathrm{re}(i+1)}[m] - \mathbf{A}_{l,m} \mathbf{b}[m] + \mathbf{u}_l^{(i)}[m] \right\|^2 \\ & \qquad + \rho \left\| \mathbf{b}_1^{(i+1)}[m] - \mathbf{b}[m] + \tilde{\mathbf{u}}_1^{(i)}[m] \right\|^2 \\ & \qquad + \rho \left\| \mathbf{b}_2^{(i+1)}[m] - \mathbf{b}[m] + \tilde{\mathbf{u}}_2^{(i)}[m] \right\|^2 \\ & \text{for } m = 0, \ldots, M-1 \end{aligned} \tag{48}$$

$$\mathbf{u}_l^{(i+1)}[m] \leftarrow \mathbf{u}_l^{(i)}[m] + \overline{\mathbf{x}}_l^{\mathrm{re}(i+1)}[m] - \mathbf{A}_{l,m} \mathbf{b}^{(i+1)}[m], \tag{49}$$

$$\tilde{\mathbf{u}}_1^{(i+1)}[m] \leftarrow \tilde{\mathbf{u}}_1^{(i)}[m] + \mathbf{b}_1^{(i+1)}[m] - \mathbf{b}^{(i+1)}[m] \tag{50}$$

$$\tilde{\mathbf{u}}_2^{(i+1)}[m] \leftarrow \tilde{\mathbf{u}}_2^{(i)}[m] + \mathbf{b}_2^{(i+1)}[m] - \mathbf{b}^{(i+1)}[m], \tag{51}$$

where $\mathbf{u}_l[m]$, $\tilde{\mathbf{u}}_1[m]$, and $\tilde{\mathbf{u}}_2[m]$ are the scaled dual vectors corresponding to the equality constraints in (44b)-(44e). The scalar ρ is the penalty parameter in the augmented Lagrangian [16]. The closed-form solutions of the problems in (45) and (48) are derived as follows:

$$\overline{\mathbf{x}}_l^{\mathrm{re}(i+1)}[m] = \frac{\rho\left(\mathbf{A}_{l,m} \mathbf{b}^{(i)}[m] - \mathbf{u}_l^{(i)}[m]\right) + \overline{\mathbf{d}}_l^{\mathrm{re}}[m]}{\rho + 1}, \quad \forall l, m \tag{52}$$

$$\begin{aligned} \mathbf{b}^{(i+1)}[m] = & \left(\sum_{l=1}^{L} \mathbf{A}_{l,m}^{\mathrm{T}} \mathbf{A}_{l,m} + 2\mathbf{I}_{K(O_{\mathrm{re}}+O_{\mathrm{im}})} \right)^{-1} \\ & \cdot \left(\sum_{l=1}^{L} \mathbf{A}_{l,m}^{\mathrm{T}} \left(\overline{\mathbf{x}}_l^{\mathrm{re}(i+1)}[m] + \mathbf{u}_l^{(i)}[m] \right) \right. \\ & \left. + \mathbf{b}_1^{(i+1)}[m] + \tilde{\mathbf{u}}_1^{(i)}[m] + \mathbf{b}_2^{(i+1)}[m] + \tilde{\mathbf{u}}_2^{(i)}[m] \right). \end{aligned} \tag{53}$$

The solutions to the problems (46)-(47) can also be obtained in closed form. However, we have observed empirically that the harsh clipping effect of the projection functions used in closed-form updates adversely affects the performance of the ADMM-based receiver. This observation aligns with our previous work [17], and we believe this is due to the harsh diminishing effect of other primal and dual optimization variables. One heuristic solution to preserve the effect of other variables' updates is to soften the projectors using their approximations with the help of sigmoid, i.e., $\mathrm{sigm}(x) = 1/(1+e^{-x})$ and softmax function, i.e., $\sigma(\mathbf{x})_j = e^{x_j}/(\sum_{j'} e^{x_{j'}})$. Using these functions, the updates in (46)-(47) are given as shown at the top of the next page.

The ADMM algorithm iteratively updates the first block of the primal variables, i.e., $\{\bar{\mathbf{x}}_l^{\mathrm{re}}[m], \mathbf{b}_1[m], \mathbf{b}_2[m]\}$, the second block of primal variables $\{\mathbf{b}[m]\}$, and the dual variables $\{\mathbf{u}_l[m], \tilde{\mathbf{u}}_1[m], \tilde{\mathbf{u}}_2[m]\}$ using (52)-(56), (49)-(51). After finding the solution to the ADMM algorithm, the soft estimates of the symbols are obtained at each subcarrier using $\bar{\mathbf{s}}^{\mathrm{re}}[m]$ and $\mathbf{b}[m]$ as $\bar{\mathbf{s}}^{\mathrm{re}}[m] = \begin{bmatrix} \mathbf{I}_K \otimes \mathbf{z}_{\mathrm{re}}^{\mathrm{T}} & \mathbf{0} \\ \mathbf{0} & \mathbf{I}_K \otimes \mathbf{z}_{\mathrm{im}}^{\mathrm{T}} \end{bmatrix} \mathbf{b}[m]$. Then, the minimum distance detector is applied to the soft estimates.

VII. Numerical Experiments

In this section, we will quantify the channel estimation error and uplink data detection in a cell-free massive MIMO system with low-resolution ADCs. The ADMM-based detector operates on the bit level, and therefore we evaluate its performance using the uncoded BER. We will compare different schemes for channel estimation and uplink data reception. We consider $L = 64$ randomly deployed APs in a $1 \times 1\,\mathrm{km}^2$ area. Each AP has $N = 4$ antennas and there are $K = 20$ randomly dropped UEs in this network area. The path loss in decibel scale is given according to Urban Microcell Street Canyon model as $-32.4 - 20\log_{10}(f_c) - 31.9\log_{10}(d) + \mathcal{N}(0, 8.2^2)$ where d is the distance between two nodes in meters, $f_c = 7.5\,\mathrm{GHz}$ is the carrier frequency, and 8.2 is the variance of the lognormal shadow fading [18, Table 7.4.1-1]. There is a $10\,\mathrm{m}$ height difference between the APs and UEs. The number of subcarriers and channel taps are $M = 512$ and $R = 5$, respectively. The subcarrier spacing is $15\,\mathrm{kHz}$. The noise variance is computed for the bandwidth of $B = 512 \cdot 15\,\mathrm{kHz} = 7.68\,\mathrm{MHz}$, and a noise figure of $7\,\mathrm{dB}$, i.e., $\sigma^2 = -98.15\,\mathrm{dBm}$. The Saleh-Valenzuela model [19] is used to model the power delay profile with $\Gamma = \gamma = 2$ and 5 clusters [20, Eqn. (7.52)]. The azimuth and elevation angles of each cluster are generated uniformly randomly from the 40° neighborhood of the nominal line-of-sight angles, and correlation matrices $\mathbf{R}_{klr}$ are generated according to the power delay profiles and uniform linear array (ULA) response vectors. The uplink transmit power is $p_k = 0.1\,\mathrm{W}\ \forall k$. The Lloyd-Max algorithm is used to determine the quantization levels.

In Fig. 1, we compare the channel estimation performance of the LS and MMSE estimators for $b = 1$-bit, $b = 2$-bit, and perfect-resolution ADCs in terms of the cumulative distribution function (CDF) of the normalized mean-square error (NMSE) for random AP and UE locations. The pilot signals are generated randomly on the unit circle. We can see that, for some AP-UE channels, the estimation quality is not so good due to both severe channel conditions and limited quantization resolution. As expected, $b = 1$-bit quantization has a more detrimental effect. On the other hand, the MMSE estimator results in smaller NMSE since it exploits the statistics of the correlated Rayleigh fading channels. In the remainder of the simulations, the MMSE estimator is utilized.

Fig. 2 shows the BER performance of different UEs (sorted from the worst to the best UE in terms of BER along the x-axis) when $b = 1$-bit ADCs are employed with QPSK modulation. Since the quantization-aware MMSE receiver requires computing a covariance matrix that lacks a closed-form expression, the BZF is presented as an alternative. The quantization-aware BZF receiver achieves improved BER performance by exploiting the 1-bit Bussgang decomposition. However, the proposed ADMM-based approach outperforms both MMSE and BZF by up to a 10-fold improvement, particularly for the lucky UEs.

In Fig. 3, we repeat the previous experiment with $b = 2$-bit ADCs. This time only the quantization-unaware MMSE receiver is shown as a benchmark since computation of Bussgang gain matrices for quantization-aware receivers requires an extensive number of Monte Carlo trials, which is not practical. We again observe that there is a huge performance improvement in the orders of magnitude with the ADMM receiver. Exploiting the modulation structure and minimizing the distance to the quantized signal, the ADMM receiver results in much better performance.

VIII. Conclusions

We have analyzed the adverse impact of low-resolution ADCs on both channel estimation and uplink data detection performance. Our study, conducted for a wideband OFDM channel, enables the implementation of both linear receivers and an ADMM-based receiver on a per-subcarrier basis. The quantization effect significantly degrades channel estimation performance, particularly for certain disadvantaged UEs. However, the proposed ADMM-based receiver achieves meaningful BER performance for most UEs by exploiting the specific structure of the constellation and accounting for quantization by minimizing the distance between the quantized signal and the unknown, unquantized noise-free signal. Compared to linear receivers, the ADMM-based approach provides orders-of-magnitude performance gains while remaining practical to implement because of its closed-form update formulas.

References

[1] H. Q. Ngo, A. Ashikhmin, H. Yang, E. G. Larsson, and T. L. Marzetta, "Cell-free Massive MIMO versus small cells," *IEEE Trans. Wireless Commun.*, vol. 16, no. 3, pp. 1834–1850, 2017.

[2] Ö. T. Demir, E. Björnson, and L. Sanguinetti, "Foundations of user-centric cell-free massive MIMO," *Foundations and Trends® in Signal Processing*, vol. 14, no. 3-4, pp. 162–472, 2021. [Online]. Available: http://dx.doi.org/10.1561/2000000109

[3] H. Q. Ngo, G. Interdonato, E. G. Larsson, G. Caire, and J. G. Andrews, "Ultradense cell-free massive MIMO for 6G: Technical overview and open questions," *Proceedings of the IEEE*, 2024.

[4] H. Masoumi and M. J. Emadi, "Performance analysis of cell-free massive MIMO system with limited fronthaul capacity and hardware impairments," *IEEE Transactions on Wireless Communications*, vol. 19, no. 2, pp. 1038–1053, 2020.

[5] X. Hu, C. Zhong, X. Chen, W. Xu, H. Lin, and Z. Zhang, "Cell-free massive MIMO systems with low resolution ADCs," *IEEE Transactions on Communications*, vol. 67, no. 10, pp. 6844–6857, 2019.

[6] Y. Zhang, M. Zhou, X. Qiao, H. Cao, and L. Yang, "On the performance of cell-free massive MIMO with low-resolution ADCs," *IEEE Access*, vol. 7, pp. 117 968–117 977, 2019.

$$\left[\mathbf{b}_1^{(i+1)}[m]\right]_j = \mathrm{sigm}\left(\left[\mathbf{b}^{(i)}[m]\right]_j - \left[\tilde{\mathbf{u}}_1^{(i)}[m]\right]_j\right) \tag{54}$$

$$\left[\mathbf{b}_2^{(i+1)}[m]\right]_{O_{\mathrm{re}}(k-1)+j} = \sigma\left(\left[\mathbf{b}^{(i)}[m] - \tilde{\mathbf{u}}_2^{(i)}[m]\right]_{O_{\mathrm{re}}(k-1)+1:O_{\mathrm{re}}k}\right)_{O_{\mathrm{re}}(k-1)+j} \tag{55}$$

$$\left[\mathbf{b}_2^{(i+1)}[m]\right]_{KO_{\mathrm{re}}+O_{\mathrm{im}}(k-1)+j} = \sigma\left(\left[\mathbf{b}^{(i)}[m] - \tilde{\mathbf{u}}_2^{(i)}[m]\right]_{KO_{\mathrm{re}}+O_{\mathrm{im}}(k-1)+1:KO_{\mathrm{re}}+O_{\mathrm{im}}k}\right)_{KO_{\mathrm{re}}+O_{\mathrm{im}}(k-1)+j}. \tag{56}$$

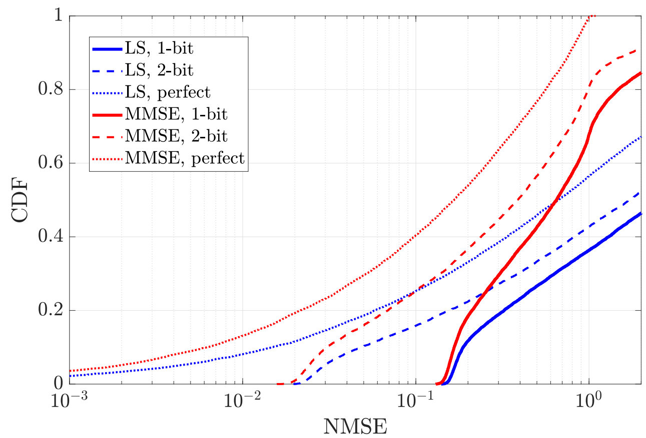

Fig. 1. The CDF of NMSE for different channel estimation schemes and number of quantization bits.

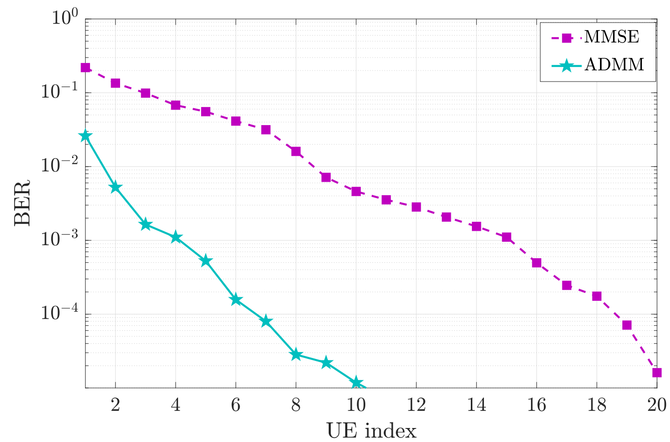

Fig. 3. The BER of $K = 20$ UEs with different receivers for $b = 2$.

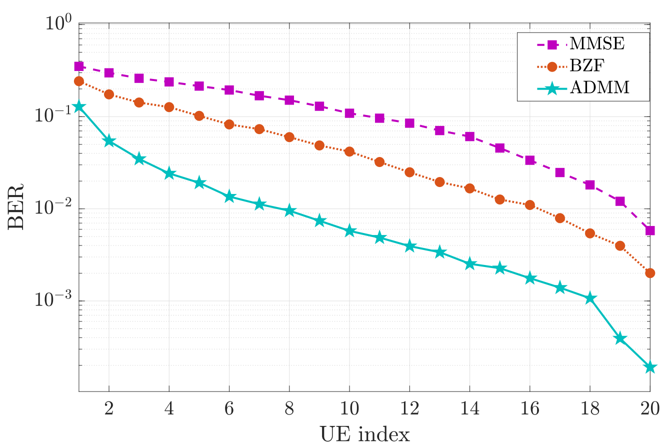

Fig. 2. The BER of $K = 20$ UEs with different receivers for $b = 1$.

[7] M. Bashar, H. Q. Ngo, K. Cumanan, A. G. Burr, P. Xiao, E. Björnson, and E. G. Larsson, "Uplink spectral and energy efficiency of cell-free massive MIMO with optimal uniform quantization," *IEEE Transactions on Communications*, vol. 69, no. 1, pp. 223–245, 2020.

[8] C. Mollén, J. Choi, E. G. Larsson, and R. W. Heath, "Uplink performance of wideband Massive MIMO with one-bit ADCs," *IEEE Trans. Wireless Commun.*, vol. 16, no. 1, pp. 87–100, 2017.

[9] C. Studer and G. Durisi, "Quantized massive MU-MIMO-OFDM uplink," *IEEE Transactions on Communications*, vol. 64, no. 6, pp. 2387–2399, 2016.

[10] S. N. Jin, D. W. Yue, and H. H. Nguyen, "Spectral efficiency of a frequency-selective cell-free massive MIMO system with phase noise," *IEEE Wireless Communications Letters*, vol. 10, no. 3, pp. 483–487, 2020.

[11] A. Pitarokoilis, E. Björnson, and E. G. Larsson, "Performance of the massive MIMO uplink with OFDM and phase noise," *IEEE Wireless Commun. Lett.*, vol. 20, no. 8, pp. 1595–1598, 2016.

[12] A. B. Üçüncü, E. Björnson, H. Johansson, A. O. Yılmaz, and E. G. Larsson, "Performance analysis of quantized uplink massive MIMO-OFDM with oversampling under adjacent channel interference," *IEEE Transactions on Communications*, vol. 68, no. 2, pp. 871–886, 2020.

[13] L. Sanguinetti, E. Björnson, and J. Hoydis, "Toward Massive MIMO 2.0: Understanding spatial correlation, interference suppression, and pilot contamination," *IEEE Transactions on Communications*, vol. 68, no. 1, pp. 232–257, 2020.

[14] L. V. Nguyen, A. L. Swindlehurst, and D. H. N. Nguyen, "Linear and deep neural network-based receivers for massive MIMO systems with one-bit ADCs," *IEEE Transactions on Wireless Communications*, vol. 20, no. 11, pp. 7333–7345, 2021.

[15] Y. Li, C. Tao, G. Seco-Granados, A. Mezghani, A. L. Swindlehurst, and L. Liu, "Channel estimation and performance analysis of one-bit massive MIMO systems," *IEEE Transactions on Signal Processing*, vol. 65, no. 15, pp. 4075–4089, 2017.

[16] S. Boyd, N. Parikh, E. Chu, B. Peleato, and J. Eckstein, "Distributed optimization and statistical learning via the alternating direction method of multipliers," *Foundations and Trends in Machine Learning*, vol. 3, no. 1, pp. 1–122, 2010.

[17] Ö. T. Demir and E. Björnson, "ADMM-based one-bit quantized signal detection for massive MIMO systems with hardware impairments," in *IEEE International Conference on Acoustics, Speech and Signal Processing (ICASSP)*, 2020, pp. 9120–9124.

[18] *5G; Study on channel model for frequencies from 0.5 to 100 GHz (Release 14)*. 3GPP TR 38.901, Jan. 2018.

[19] A. A. Saleh and R. A. Valenzuela, "A statistical model for indoor multipath propagation," *IEEE J. Sel. Areas Commun.*, vol. 5, no. 2, pp. 128–137, 1987.

[20] E. Björnson and Ö. T. Demir, *Introduction to multiple antenna communications and reconfigurable surfaces*. Now Publishers, Inc., 2024.